

Extended Identification-Based Predictive Control for adaptive impact mitigation

Cezary GRACZYKOWSKI^{✉*} and Rami FARAJ[✉]

Institute of Fundamental Technological Research PAS, Pawińskiego 5B, 02-106 Warszawa, Poland

Abstract. The paper introduces Extended Identification-Based Predictive Control (EIPC), which is a novel control method developed for the problem of adaptive impact mitigation. The model-based approach utilizing the paradigm of Model Predictive Control is combined with sequential identification of selected system parameters and process disturbances. The elaborated method is implemented in the shock-absorber control system and tested under impact loading conditions. The presented numerical study proves the successful and efficient adaptation of the absorber to unknown excitation conditions as well as to unknown force and leakage disturbances appearing during the process. The EIPC is used for both semi-active and active control of the impact mitigation process, which are compared in detail. In addition, the influence of selected control parameters and disturbance identification on the efficiency of the impact absorption process is assessed. As a result, it can be concluded that an efficient and robust control method was developed and successfully applied to the problem of adaptive impact mitigation.

Key words: adaptive control; optimal control; predictive control; impact mitigation; shock absorber.

1. INTRODUCTION

The problem addressed within the paper refers to impact mitigation, which is a process aimed at alleviation of loading acting on the amortized objects with a requirement to absorb and dissipate the entire excitation energy. Devices applied for this purpose are called shock-absorbers and they can be found in various branches of engineering, beginning from the automotive [1–3] and aerospace industry [4, 5], by off-shore protection [6], robotics [7], ending with everyday life applications, e.g., bicycle suspensions [8]. Since impact absorption in the case of the above applications lasts from several to tens of milliseconds the practical implementation of semi-active or active control methods remains very challenging. Because of that, most of all the passive absorbers were used and they are still being developed, e.g. in the form of an elastomer-filled composite tube [9] or variable-area fluid-filled tube with fluid outflow [10].

Taking advantage of the technological progress in the field of sensors and actuators, as well as data acquisition and signal processing, it becomes increasingly popular to replace typical passive absorbers with more sophisticated controlled solutions. They include magnetorheological [11, 12], and electrorheological [13] dampers, fluid absorbers with piezoelectric valves [14], devices utilizing shape memory alloys [15], and dampers based on the application of granular material [16, 17]. Apart from high performance, the above applications have also additional capabilities, such as energy harvesting [18, 19], which ensures that a part of excitation energy can be retrieved and reused.

*e-mail: cezary.graczykowski@ippt.pan.pl

Manuscript submitted 2023-01-11, revised 2023-04-13, initially accepted for publication 2023-05-09, published in August 2023.

The first semi-active and active shock absorbers utilized classical controllers, such as PID [20] with feedback to generated force or acceleration [21, 22]. In order to determine the appropriate input for the controller, the inverse dynamics problems were solved before or at the very beginning of the process [23]. Alternatively, the state-dependent path-tracking approach [24–26] with kinematics-based feedback was applied to guarantee successful and efficient impact mitigation. Further development of adaptive absorbers included the application of well-established Model Predictive Control (MPC) [27, 28]. The paper continues this approach but the MPC is combined with repeatedly performed identification of unknown process parameters. Such an approach was introduced in [29], where Identification-Based Predictive Control was elaborated to provide adaptive impact absorption under the presence of unknown disturbance forces. The presented study constitutes the next step of research, where the Extended Identification-Based Predictive Control method is established and successfully applied for extended cases of simultaneously unknown amortized object mass, disturbance force, and gas leakage.

2. PROBLEM FORMULATION

Despite the fact that impact absorption problems often concern complex mechanical systems, the development of a novel impact mitigation method is usually started using a relatively simple 1-DOF system as shown in Fig. 1.

Here the object of mass M and initial velocity v_0 is amortized by the double-chamber pneumatic absorber filled with operational gas, whose parameters are described by pressure p , temperature T , mass m , and volume V . The index of the gas parameters is “1” in a decompressed chamber and “2” in a compressed chamber. Displacement of the absorber piston is denoted by x

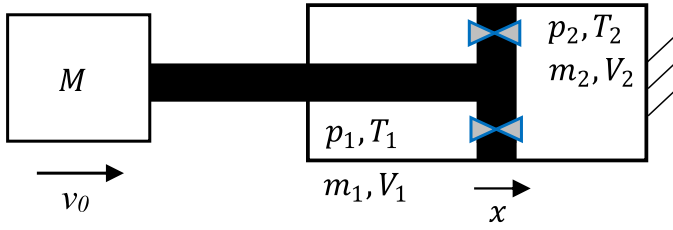


Fig. 1. Scheme of the pneumatic double-chamber absorber with controllable valve under impact excitation

and its velocity by v . The kinematics of the piston is influenced by pneumatic force $F_p(p_1, p_2)$ resulting from pressure difference appearing between the absorber chambers and by delimiting force acting on the piston at the end of the stroke F_{del} . The flow of gas between the chambers is described by the definition of the mass flow rate Q_m , which depends on pressures in both chambers p_1 and p_2 , the temperature of the gas in the upstream chamber T_{up}^c and the actual area of the flow A_v . To demonstrate the outstanding performance of the developed control method, the unknown disturbance force $F_{dist}(t)$ and unknown gas leakage $Q_{dist}(t)$ are introduced into the system model.

Applying mathematical models discussed in detail in the literature, e.g. [25], a state-space description of the system can be developed and transformed into the following form:

$$\frac{dx}{dt} = v, \quad (1)$$

$$\frac{dv}{dt} = -\frac{F_p(p_1, p_2) + F_{dist}(t) + F_{del}}{M}, \quad (2)$$

$$\frac{dp_1}{dt} = \frac{\kappa}{V_1} [-p_1 \dot{V}_1 + Q_m(p_1, p_2, T_{up}^c, A_v) RT_{up}^c + Q_{dist}(t) RT_{up}^d], \quad (3)$$

$$\frac{dp_2}{dt} = \frac{\kappa}{V_2} [-p_2 \dot{V}_2 - Q_m(p_1, p_2, T_{up}^c, A_v) RT_{up}^c - Q_{dist}(t) RT_{up}^d], \quad (4)$$

$$\frac{dm_1}{dt} = Q_m(p_1, p_2, T_{up}^c, A_v) + Q_{dist}(t), \quad (5)$$

$$\frac{dA_v}{dt} = \frac{k_v u - A_v}{T_v}. \quad (6)$$

The above system of differential equations must be supplemented by:

- initial conditions: $x(0) = x_0$, $v(0) = v_0$, $p_1(0) = p_{10}$, $p_2(0) = p_{20}$, $m_1(0) = m_{10}$, $A_v(0) = A_v^0$,
- definition of the pneumatic force $F_p = p_2 A_2 - p_1 A_1$, where A_1 and A_2 are areas of the piston,
- mass conservation equation $m_1 + m_2 = m_0 = \text{const.}$,
- definition of chamber volumes $V_1 = V_{10} + A_1 x$, $V_2 = V_{20} - A_2 x$,
- ideal gas law $p_i V_i = m_i R T_i$, $i = 1, 2$,
- relations for the temperature in the upstream chamber for controlled gas flow T_{up}^c and gas leakage T_{up}^d :

$$T_{up}^c = \begin{cases} T_2 & \text{for } A_v \geq 0, \\ T_1 & \text{for } A_v < 0; \end{cases} \quad (7a)$$

$$T_{up}^d = \begin{cases} T_2 & \text{for } p_2 \geq p_1, \\ T_1 & \text{for } p_2 < p_1. \end{cases} \quad (7b)$$

Equations (1)–(2) describe the dynamics of the amortized object, (3)–(4) define thermodynamic energy balance for the compressed and decompressed chamber, (5) defines the mass flow rate of gas between the chambers, whereas (6) corresponds to the operation of the controllable valve, which is aimed at providing an appropriate area of valve opening A_v for gas exchange.

The quantity Q_m at the r.h.s. of the flow equation (5) is formulated using the isentropic flow model, the model based on the C-b relationship (ISO 6358), or experimentally obtained characteristics. The proposed flow model assumes that the applied valve opening area can take both positive and negative values. Positive values of the valve opening area correspond to spontaneous gas flow between the chambers, which occurs in a semi-active system. It has a direct physical interpretation as a minimal area of the fluid flow inside the valve. In contrast, the negative valve opening area, which appears in the case of active control, reveals only the fact that enforced pumping of gas from decompressed to the compressed chamber is required during the process. The negative value of valve opening area has no direct physical meaning. However, it can be interpreted as a quantity correlated with the required intensity of gas pumping and the energy required for the gas pumping.

The valve area A_v is coupled with the control signal u using the classical first-order equation (6) with gain k_v and time constant T_v . According to experimental research conducted at IPPT PAN, such an approach is appropriate for the description of fast piezoelectric valves analyzed within this study.

The performance of shock absorbers is typically evaluated by measurement of maximum reaction force [22], impact absorption efficiency, or decelerations acting on the amortized object [30]. Concerning the optimal control problem, it is more convenient to formulate an integral objective function, as proposed in [29]. Here, we consider the objective function which contains the term indicating a global error of state-dependent path-tracking process and the term indicating global control cost multiplied by arbitrary weighting coefficient q :

$$J(u) = \int_0^T \left(\dot{v}(u, t) - \frac{v^2(u, t)}{2(d - x(u, t))} \right)^2 + q A_v(u, t)^2 dt. \quad (8)$$

The first term is expressed as a difference in the actual acceleration of the amortized object \dot{v} and optimal deceleration value specified for the remaining part of the process. The optimal deceleration is calculated using the object actual velocity v and the remaining part of the absorber stroke $d - x$, which always remains larger than zero due to the presence of delimiting force F_{del} , which assumes a nonzero value in the case when the piston hits the absorber bottom. In turn, the end time of the process T corresponds to the static equilibrium conditions. The second term of the objective function is expressed using the actual valve opening area A_v . The weighting coefficient q allows us to differentiate and compare semi-active and active systems

according to the following relation:

$$q = \begin{cases} \bar{q} & \text{for } A_v < 0 \quad \text{active operation,} \\ 0 & \text{for } A_v \geq 0 \quad \text{semi-active operation.} \end{cases} \quad (9)$$

Moreover, it can be used to provide a balance between the importance of the state-dependent path-tracking error and the control effort.

Finally, the optimal control problem corresponding to the adaptive impact mitigation can be formulated as follows:

$$\begin{aligned} & \text{Minimize } J(u) \text{ with respect to } u(t) \in [u_{\min}, u_{\max}] \\ & \text{subject to (1)–(6) and } \int_{x_0}^{x(T)} F_{\text{abs}}(p_1, p_2, t) dx = E_{\text{imp}}, \end{aligned} \quad (10)$$

where the absorber force $F_{\text{abs}} = F_p + F_{\text{dist}}$ and the impact energy $E_{\text{imp}} = 1/2Mv_0^2$. The last constraining equation is the condition of energy dissipation, which corresponds to the stopping of the impacting object within the available absorber stroke.

The above formulation is a complex variational problem and cannot be solved either analytically or numerically, because the mass of an amortized object as well as system disturbances are unknown. Therefore, the authors develop a dedicated control method, which is discussed in detail in the following sections.

3. DEVELOPMENT OF THE EIPC

The EIPC can be considered as a kind of Adaptive Model Predictive Control, which was developed by the authors to provide self-adaptive operation of a pneumatic absorber with automatic adjustment to actual impact conditions and compensation of disturbances. The proposed EIPC method enables an approximate solution of the formulated variational problem of adaptive impact mitigation (10) under the assumption that the mass of the impacting object M as well as functions defining system disturbances F_{dist} and Q_{dist} are not a priori known. In such a case the introduced state-space model (1)–(6) cannot be directly used to determine optimal control and optimize system response.

The proposed approach utilizes methods of system identification to construct and update the predictive model, which serves for the approximate simulation of the system dynamics. Such a model is used to determine the optimal control at assumed prediction intervals of arbitrary length. According to the paradigm of the AMPC, the procedure of system identification, update of the predictive model, and finding optimal control is repeated at each control step.

3.1. System identification

The proposed method of system identification aimed at updating the predictive model utilizes two basic approaches:

- Determination of the equivalent parameters which compensate simultaneous occurrence of unknown system parameters and disturbances.
- Identification and prediction of future changes in disturbances occurring during the process.

The first method is used when both the unknown system parameter and disturbance function appear within a single state equation. Here, it is applied for replacing unknown impacting object mass M and unknown force F_{dist} by equivalent mass parameter M_{eq} , which is defined using the actual values of pneumatic force and acceleration:

$$M_{\text{eq}}(t_i) = -\frac{F_p(t_i)}{\dot{v}(t_i)}. \quad (11)$$

In the undisturbed process the parameter M_{eq} equals to the real value of impacting object mass, while in the process with additional disturbances, it changes at the subsequent control steps in order to compensate their occurrence.

The second method is used when only one unknown disturbance function arises in a single equation of state. Here, it is applied for predicting the time history of fluid leakage between the chambers during the process. Initially, the value of fluid leakage at each control step is identified separately with the use of energy balance equations and flow equations in order to obtain three quantities:

$$\begin{aligned} \bar{Q}_{\text{dist}}^{-1}(t_i) &= \frac{\dot{p}_1(t_i)(V_{10} + A_1x(t_i))}{\kappa RT_{\text{up}}^d(t_i)} \\ &+ \frac{p_1 A_1 v(t_i)}{RT_{\text{up}}^d(t_i)} - Q_m(t_i) \frac{T_{\text{up}}^c(t_i)}{T_{\text{up}}^d(t_i)}, \end{aligned} \quad (12)$$

$$\begin{aligned} \bar{Q}_{\text{dist}}^{-2}(t_i) &= -\frac{\dot{p}_2(t_i)(V_{20} - A_2x(t_i))}{\kappa RT_{\text{up}}^d(t_i)} \\ &+ \frac{p_2 A_2 v(t_i)}{RT_{\text{up}}^d(t_i)} - Q_m(t_i) \frac{T_{\text{up}}^c(t_i)}{T_{\text{up}}^d(t_i)}, \end{aligned} \quad (13)$$

$$\bar{Q}_{\text{dist}}^{-3}(t_i) = \frac{d}{dt} \left(\frac{pV}{RT} \right) (t_i) - Q_m(t_i). \quad (14)$$

Since each identification requires measurement of different state variables and computation of different time derivatives, the computed values of fluid leakage may vary. The final value to be used in further computations can be selected from the two closest results or by their averaging. Then, the values identified at all previous control steps are used to determine the actual form of the continuous function describing the change of fluid leakage:

$$\bar{Q}_{\text{dist}}(t_i, t) = f_i(Q_{\text{dist}}(t_1), Q_{\text{dist}}(t_2), \dots, Q_{\text{dist}}(t_i), t), \quad (15)$$

which can be extrapolated to the next prediction interval.

Eventually, the predictive model applied at each control step contains two fundamental equations of the main model (1) and (6), an equation of impacting object motion that utilizes the actual value of equivalent mass $M_{\text{eq}}(t_i)$ as well as equations of energy balance and flow equation which utilize actual prediction of the fluid leakage function $\bar{Q}_{\text{dist}}(t_i, t)$:

$$\frac{dv}{dt} = -\frac{F_p(p_1, p_2)}{M_{\text{eq}}(t_i)}, \quad (16)$$

$$\frac{dp_1}{dt} = \frac{\kappa}{V_1} \left[-p_1 \dot{V}_1 + Q_m(u) RT_{\text{up}}^c + \bar{Q}_{\text{dist}}(t_i, t) RT_{\text{up}}^d \right], \quad (17)$$

$$\frac{dp_2}{dt} = \frac{\kappa}{V_2} \left[-p_2 \dot{V}_2 - Q_m(u) RT_{up}^c - \bar{Q}_{dist}(t_i, t) RT_{up}^d \right], \quad (18)$$

$$\frac{dm_1}{dt} = Q_m(u) + \bar{Q}_{dist}(t_i, t). \quad (19)$$

3.2. Reformulation and solution of the control problem

In the EIPC method, the formulated variational optimization problem defined by (10) is decomposed into a series of standard path-tracking problems starting at the beginning of each control step and aimed at finding actual optimal control using an updated predictive model of the system. Thus, the solution is obtained by sequential solving of the control problems formulated as follows:

$$\text{Minimize: } J(u) = \int_{t_i}^T \left(\dot{v}(u, t) - \frac{v(t_i)^2}{2(d-x(t_i))} \right)^2 + qA_v(u, t)^2 dt$$

with respect to: $u(t) \in [u_{\min}, u_{\max}]$,

$$\text{subject to: (1), (6), (16)–(19), } \int_{x_0}^{x(T)} F_p(p_1, p_2, t) dx = E_{imp}. \quad (20)$$

In the considered case when the absorber stroke d is close to the length of the compressed chamber, the condition of energy dissipation can be always fulfilled at the end of the process when the infinitesimal mass of the gas remains in the compressed chamber and the application of infinitesimal control allows to obtain the state of static equilibrium. Thus, the condition of energy dissipation can be omitted and the prediction interval can be arbitrarily shortened. In particular, it can be limited to a length of a single control step in order to speed up the computations.

Despite the applied decomposition and control horizon shortening the proposed iterative method provides an approximation of the global solution of the original control problem. Such a feature is provided since each of the sequentially solved control problems includes the optimal value of acceleration for the entire remaining part of the process. A better approximation of the global solution requires obtained in advance knowledge about changes of disturbances in time, which is impossible in practice.

The solution to the control problem defined by (20) can be obtained using Pontryagin's maximum principle or direct methods based on discretization of the control function in the time domain, but in both cases, the related difficulty is the indefinite time horizon of the process. Herein, we adopt a different approach and apply either continuous control with parametrization of the control signal using the polynomial function or digital control with the constant value of the control signal. In the latter case, the original dynamic optimization problem solved at each control step is reduced to a one-dimensional static optimization problem:

$$\text{Find } u^{\text{opt}} = \arg \min \int_{t_i}^{t_i+\Delta t} \left(\dot{v}(u) - \frac{v(t_i)^2}{2(d-x(t_i))} \right)^2 + qA_v(u)^2 dt. \quad (21)$$

Let us note that the equation governing valve response is independent of other equations and has the analytical solution:

$$A_v(t) = A_v(t_i) e^{-\frac{(t-t_i)}{T_0}} + A_v^{\max} \frac{u}{u_{\max}} \left(1 - e^{-\frac{(t-t_i)}{T_0}} \right) \quad \text{for } u \geq 0 \text{ and } k_v = \frac{A_v^{\max}}{u_{\max}}, \quad (22)$$

$$A_v(t) = A_v(t_i) e^{-\frac{(t-t_i)}{T_0}} + A_v^{\min} \frac{u}{u_{\min}} \left(1 - e^{-\frac{(t-t_i)}{T_0}} \right) \quad \text{for } u < 0 \text{ and } k_v = \frac{A_v^{\min}}{u_{\min}}. \quad (23)$$

Thus, the parameterization of the control signal u corresponds to the parameterization of the valve opening A_v and the differential equation governing valve operation does not have to be included within the numerical solution of the optimization problem. Moreover, it can be proved that the objective function of the formulated optimization problem is convex in terms of control variable so the solution can be found using standard gradient-based methods at small numerical cost.

4. STUDY ON PERFORMANCE OF THE EIPC

The presented numerical examples are aimed at proving the effectiveness of the EIPC method in the mitigation of the impact of a single object with unknown mass and initial velocity. The considered process disturbances include unknown elastic force occurring during the entire process and unknown gas leakage appearing at its middle part. However, neither the type of disturbances, the time of their occurrence, nor their characteristics are known for the control system.

The subsequent numerical examples reveal how the impact mitigation process is influenced by valve parameters, the applied control type (semi-active vs. active), and the control cost. The values of system parameters, which were applied in numerical simulations are collected in Table 1.

Table 1
Parameters applied in the numerical examples

M (kg)	v_0 (m/s)	p_{10}, p_{20} (kPa)	A_1, A_2 (mm ²)
5	5	300	1256.64
V_{10} (cm ³)	V_{20} (cm ³)	d (mm)	T_{10}, T_{20} (K)
7.54	118.12	94	293.15

The implemented model of a double-chamber pneumatic cylinder utilizes the classical isentropic flow model which describes the subcritical and critical flow conditions using the St.-Venant function. According to this model, the mass flow rate of gas between the upstream chamber (2) and downstream cham-

ber (1) is defined as:

$$Q_m(p_1, p_2, T_2, A_v) = CA_v(t) \frac{p_2}{\sqrt{RT_2}} \sqrt{\frac{2\kappa}{\kappa-1} \left(q^{\frac{2}{\kappa}} - q^{\frac{\kappa+1}{\kappa}} \right)}, \quad (24)$$

$$q = \begin{cases} \frac{p_1}{p_2} & \text{for } p_2 < p_1 \left(\frac{2}{\kappa+1} \right)^{\frac{\kappa}{1-\kappa}}, \\ \left(\frac{2}{\kappa+1} \right)^{\frac{\kappa}{\kappa-1}} & \text{for } p_2 \geq p_1 \left(\frac{2}{\kappa+1} \right)^{\frac{\kappa}{1-\kappa}}, \end{cases} \quad (25)$$

where C is a discharge coefficient and κ is an adiabatic exponent. The critical ratio of pressures which defines the subcritical and critical flow range is calculated for the air ($\kappa = 1.4$) and equals approximately 0.5283.

4.1. A system with unknown mass and force disturbance

The first numerical example concerns control of the system with unknown impacting object mass and force disturbance, but without fluid leakage. The example has two main objectives: i) demonstration of the effectiveness and robustness of the EIPC method, ii) analysis of the system response for piezoelectric valves of various operation speeds and constrained maximal flow areas.

The operation of the control system is based on the computation of the equivalent mass according to (11), identification of fluid leakage according to (12)–(14), which is here close to zero, and repetitive solution of the updated optimization problem at the subsequent control steps. The control cost is neglected ($q = 0$) since negative valve areas are not expected.

The results in Fig. 2 present the operation of control executed using piezoelectric valves of various operation speeds specified by the constant T_v . The application of digital control with a fast piezoelectric valve results in a system response resembling the theoretical optimal solution [25], in which the force increases at the maximal rate, then is maintained constant, and finally decreases at the end of the process, causing dissipation of the entire impact energy.

In particular, for the fast piezoelectric valve with a time constant $T_v = 0.5$ ms the second stage of the process includes a gradual decrease of the applied optimal control signal and gas flow area from their maximal values (not achieving u^{\max} and A_v^{\max}) to the values being close to zero. The corresponding generated force is maintained approximately constant and visible oscillations appear only at the end of the process (Fig. 2a–c – navy lines).

Application of a slower piezoelectric valve with a time constant $T_v = 2$ ms (Fig. 2a–c – red lines) results in a still satisfactory but clearly worse response of the impact absorbing system, which includes two unfavorable phenomena. Firstly, at the beginning of the second stage, the applied optimal control signal achieves its limit value, the increase of gas flow area is insufficient, which causes an excessive increase in the generated force. Secondly, during a further part of the second stage, the value

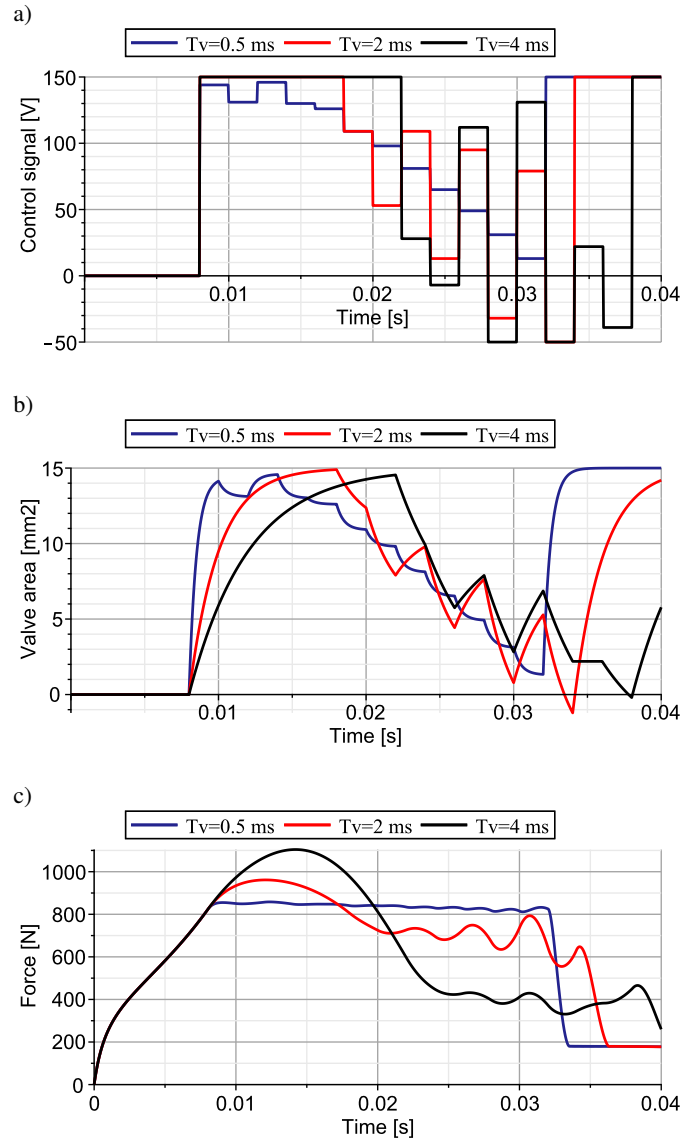


Fig. 2. Control of pneumatic damper using piezoelectric valves of various time constants T_v : a) applied control signal, b) resulting valve opening area, c) generated force

of the applied control signal commutatively increases and decreases, which results in the opening and closing of the valve and corresponding oscillations of the generated force.

Finally, the application of the slowest piezoelectric valve with a time constant $T_v = 4$ ms (Fig. 2a–c – black lines) causes evidently non-satisfactory response of the system in which force heavily increases at the initial part of the process and further, it is maintained constant at a low level with substantial oscillations. Nevertheless, the initial excessive force increase can be eliminated by the application of the valve of the same time constant but larger maximal flow area, see Fig. 3.

The above-discussed simulations of the EIPC operation enable a comparison of the obtained change of generated force with general requirements for the designed impact-absorbing system. The procedure allows for the selection of the piezoelectric valve of a proper time constant and maximal flow area.

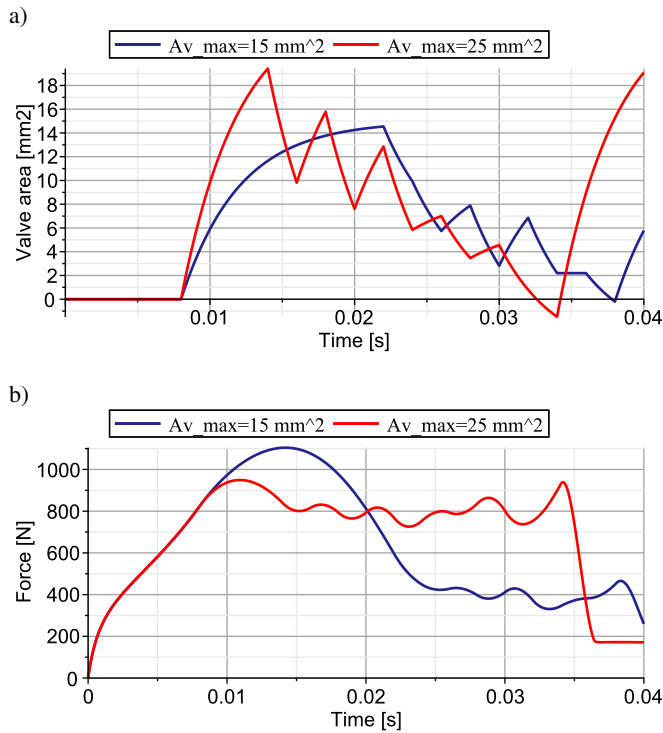


Fig. 3. Control of pneumatic damper using slow piezoelectric valve of various maximal flow areas A_v^{\max} : a) valve opening area, b) resulting generated force

4.2. A system with unknown mass, force disturbance, and leakage disturbance

The second numerical example concerns the control of the impact scenario with unknown impacting object mass, force, and leakage disturbance. The main objectives of the example are i) to compare the operation of the semi-active and active control system without leakage identification, and ii) to investigate the influence of leakage identification on the operation of both control strategies, system efficiency, and robustness.

Similarly, as in the previous case, the control system operation is based on the determination of the equivalent mass and repetitive solution of the updated control problem at subsequent control steps. The time constant for semi-active and active systems is assumed as $T_v = 0.5$ ms, which provides sufficient speed for piezoelectric valve operation and efficient gas pumping. The control cost is neglected ($q = 0$) in order to achieve the highest efficiency of the path-tracking process. The leakage disturbance includes fluid flow from the compressed to the decompressed chamber, which starts at $t = 0.015$ s, increases to maximal value at $t = 0.016$ s, and then decreases to zero value at $t = 0.019$ s.

The results presented in Fig. 4 show the operation of semi-active and active control in the case of leakage not identified and taken into account in the predictive model of the system.

At the beginning of leakage occurrence, the operation of both methods is identical. At the end of the control step with leakage occurrence ($t = 0.016$ s), both control systems detect sudden changes in system kinematics and significantly update the actual value of optimal deceleration. As a result of optimal control re-computation, the control signal is reduced to a small value

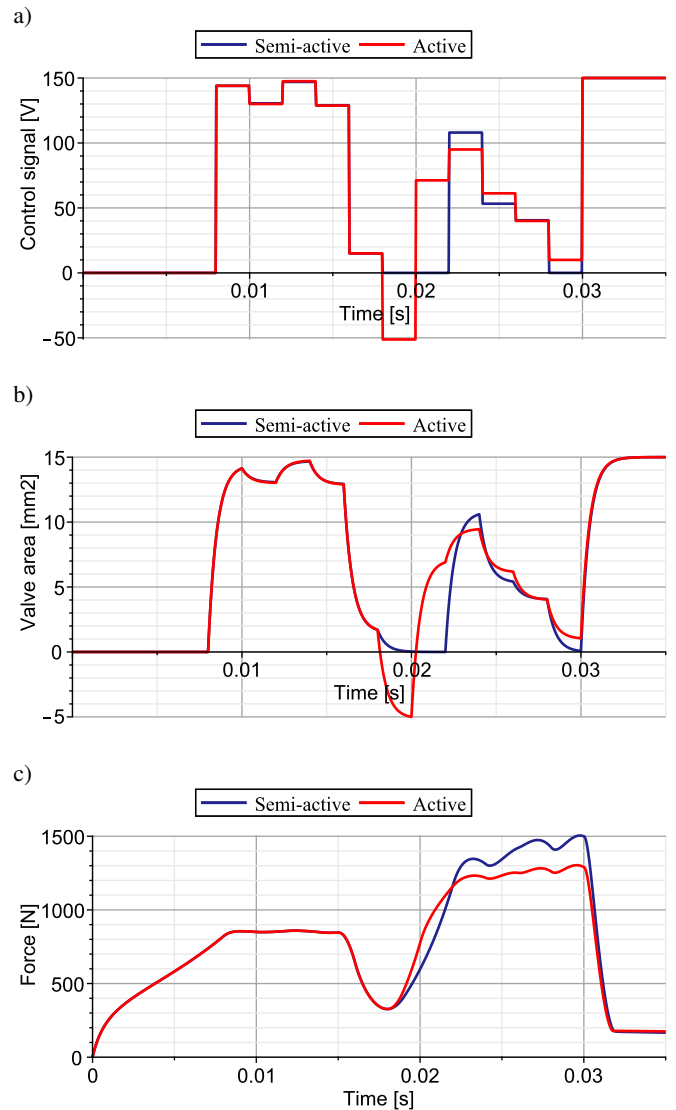


Fig. 4. Control of pneumatic damper with the use of semi-active and active control without leakage identification: a) applied control signal, b) resulting valve opening area, c) resulting generated force

(Fig. 4a), and the corresponding valve closing process is executed (Fig. 4b).

At the subsequent control steps, the update of the system path and control computation is repeated, but the action of both control systems is entirely different. In the semi-active system, the zero control signal is applied and the valve remains closed for two consecutive control steps until the optimal deceleration level and the corresponding generated force level are reached (Fig. 4a-c – navy lines). In contrast, in the active system the applied negative value of the control signal results in the pumping of gas to the compressed chamber, which ensures a faster increase of total generated force and reaching the optimal value in a shorter time (Fig. 4a-c – red line). The consequence is a lower value of reaction force during the remaining part of the process.

The results presented in Fig. 5 show the operation of semi-active and active control systems in the case when leakage is identified and included in the predictive model. At the end of the

Extended Identification-Based Predictive Control for adaptive impact mitigation

control step with leakage occurrence ($t = 0.016$ s), both control systems detect the change of system kinematics, and additionally, the value of leakage is estimated using state measurements and equations (12)–(14). Since only a single identification point is available, the constant value of leakage is assumed and introduced into the energy balance and flow equations of the predictive model. Application of a more accurate predictive model complemented by expected leakage value results in the more precise computation of the optimal control. The consequence is a better response of the control system to occurring disturbance and immediate reduction of the control signal to the lowest possible value (Fig. 5a). In the semi-active system it results in faster closing of the valve and maximal possible reduction of force decrease (Fig. 5b–c – navy lines). In turn, in the active system, it causes intensive gas pumping leading to a fast reduction of force drop and its increase before the end of the control step (Fig. 5b–c – red lines).

At the subsequent control steps, the leakage identification is conducted again, which gives additional identification data and

allows us to predict the future change in leakage more precisely. Computation of the optimal control with the use of an updated predictive model results in different operations of semi-active and active control systems. In the semi-active system, the valve remains closed for the next two control steps in order to reach the optimal deceleration and force level (Fig. 5a–c – navy lines). In contrast, in the active system, the gas pumping must be gradually reduced and the optimal system path is reached in one control step (Fig. 5a–c – red lines). As a result, the active control system allows us to obtain lower values of reaction force during the remaining part of the process.

The comparison of the plots of generated forces in semi-active and active systems without leakage identification (Fig. 4c) and with leakage identification (Fig. 5c) reveals the significantly better performance of the latter ones. The ordered sequence of control systems of increasing performance includes: i) semi-active systems, ii) semi-active systems with leakage identification, iii) active systems, and iv) active systems with leakage identification. The presented analysis and simulation results allow us to choose the proper type of system for a given application in order to fulfill assumed requirements on robustness to leakage disturbance.

4.3. Influence of the control cost

The third numerical example concerns control of the pneumatic damper under an impact scenario involving unknown impacting object mass, force, and leakage disturbances, taking into account the control cost. The objective of the example is to investigate the influence of the weighting coefficient of the control cost on the calculated optimal control signal, the corresponding valve opening, and the change of force generated by the absorber.

The operation of the considered control system is analogous as previously; it is based on the identification of unknown parameters and repetitive solutions of the updated optimization problem at each control step. However, in the case of leakage occurrence causing active response with gas pumping, the objective function of the optimization problem (20) is affected by the control cost term, which influences the calculated solution. In order to enable its comparison with solutions obtained for previously considered semi-active and active systems and neglecting the control cost, the parameters of the valve and disturbances are the same as in previous simulations.

The numerical results presented in Fig. 6 show the applied control signal, the valve opening area, and the absorber reaction force for three control systems with different values of the weighting coefficient q of the control cost term. During the initial stage of the process, the operation of all control systems and the corresponding response of the pneumatic absorber are identical since the value of the valve opening area remains positive. However, the influence of the control cost becomes clearly visible after time $t = 0.016$ s, when the leakage is detected. In the case when the weighting coefficient q is relatively low (approx. up to $50 \cdot 10^{12}$) the applied control signal, the corresponding valve opening, and the resulting system response are similar to the active control system without control cost, cf. Figs. 5 and 6 – red lines. In particular, during the first control step after leak-

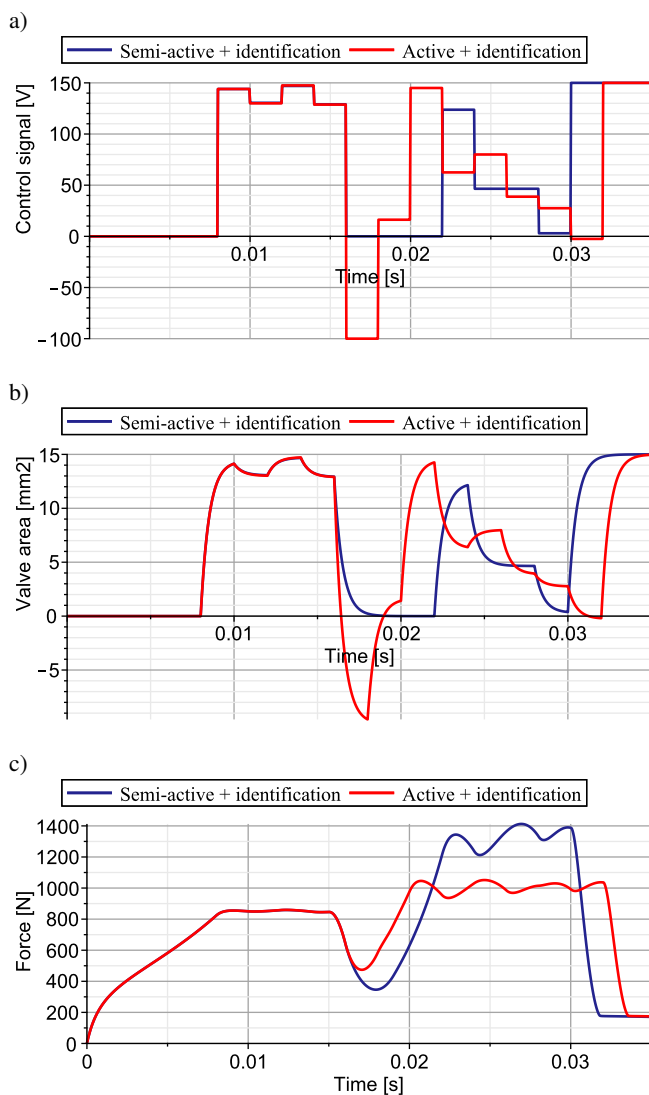


Fig. 5. Control of pneumatic damper with the use of semi-active and active control with leakage identification: a) applied control signal, b) resulting valve opening area, c) generated force

age detection, the control signal is reduced to a minimal value in order to achieve maximal negative valve opening indicating intensive gas pumping and the fastest possible increase of generated force (Fig. 6a–c – red lines).

In contrast, when the weighting coefficient q is relatively high (approx. above $10000 \cdot 10^{12}$). The operation of the control system is strongly affected by the control cost and the negative values of the valve opening area are avoided. As a result, the applied control signal and system response clearly resemble the case of a semi-active control system, cf. Figs. 5 and 6 – navy lines. In such a case, the valve remains closed for several control steps in order to achieve the required level of reaction force, which now becomes significantly higher (Fig. 6a–c – navy lines).

Eventually, in the case of the intermediate value of the weighting coefficient q of the control cost term (approx. in the range of $50 \cdot 10^{12}$ – $10000 \cdot 10^{12}$), the operation of the control

system and absorber response are located between previously considered extreme cases. In particular, after leakage detection, the intermediate negative value of the control signal and corresponding valve opening area is applied (Fig. 6a–b – black lines). Consequently, the level of force generated after the end of leakage is located between the values obtained for active and semi-active control systems (Fig. 6c – black line).

The proposed methodology and conducted simulations allow us to choose the proper value of the weighting coefficient of the control cost for the expected range of impact conditions and leakage disturbance. The appropriately selected value of the weighting coefficient q can be used to provide a relevant compromise between active control with high control cost providing low values of impacting object deceleration, and semi-active control, which is energy-efficient but results in higher deceleration values.

4.4. Assessment of impact absorption effectiveness

In order to quantitatively assess the effectiveness of impact absorption, the coefficient of impact absorption efficiency η is introduced. It is defined as:

$$\eta = \frac{\int_0^{x_{\max}} F_{\text{abs}}(x) dx}{F_{\max} x_{\max}}, \quad (26)$$

where the numerator denotes absorbed energy, while the denominator indicates the amount of energy that can be absorbed using the maximal generated value of reaction force F_{\max} and utilized part of the absorber stroke x_{\max} . Since the proposed adaptive system always provides absorption of the entire impact energy (cf. equation (10)) the integral in the numerator equals to initial kinetic energy of the impacting object. Moreover, in order to ensure process optimality, the control system provides that the entire stroke of the absorber is utilized $x_{\max} = d$. Thus, in the considered case the definition of the impact absorption efficiency coefficient takes the simplified form:

$$\eta = \frac{1}{2} \frac{M v_0^2}{F_{\max} d} = \frac{F_{\text{opt}}}{F_{\max}}, \quad (27)$$

and it denotes the ratio of the theoretical optimal value of force F_{opt} and maximal value of the reaction force obtained from the numerical simulation F_{\max} .

Let us note that optimal impact absorption with the constant optimal value of generated reaction force (and the corresponding value of $\eta = 1$) is purely theoretical since it corresponds to the application of the active control system with enormous efficiency, which reacts infinitely fast on the occurrence of force disturbance or fluid leakage. In the considered case of a pneumatic damper, the coefficient of impact absorption efficiency depends on the value of initial pressure inside the pneumatic cylinder, which determines the change of reaction force during the first stage of the process, the corresponding length of this stage and the required level of force during the second stage. Moreover, the coefficient η is strongly affected by the leakage of the gas between the chambers, which occurs during the pro-

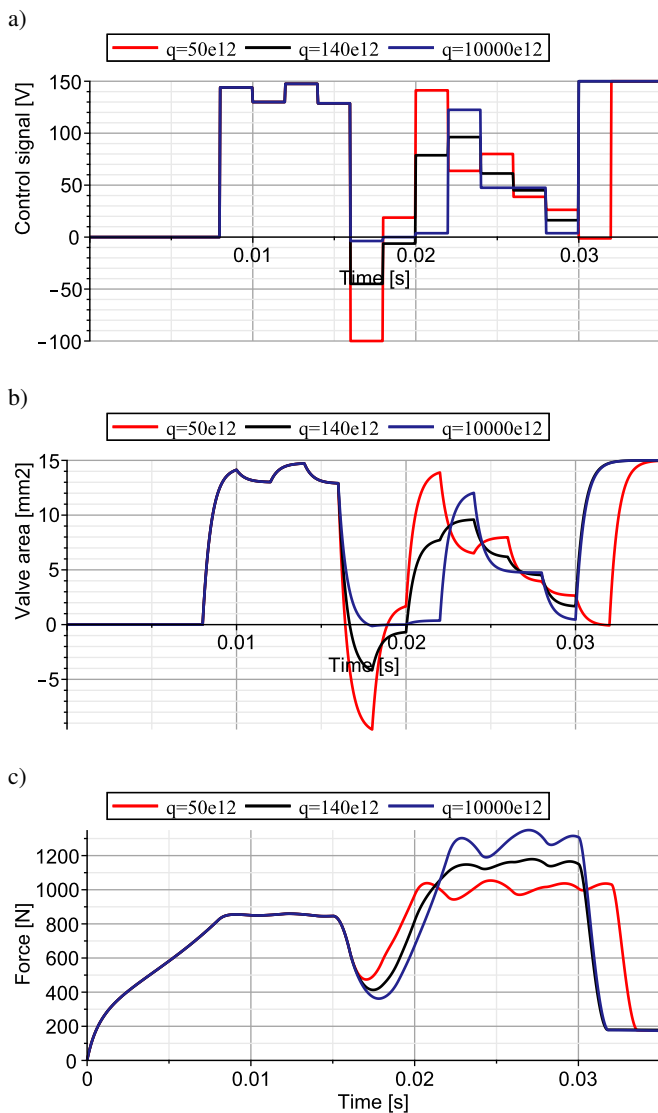


Fig. 6. Control of pneumatic damper with the use of active control with various weighting coefficients of the control cost term a) applied control signal, b) resulting valve opening area, c) resulting total generated force

Extended Identification-Based Predictive Control for adaptive impact mitigation

cess and its assumed intensity. Thus, the obtained values of η are expected to be significantly smaller than 1.

The values of impact absorption efficiency coefficients were computed and compared for each system analyzed in previously presented numerical examples, see Table 2. The conducted computations reveal that for the system with unknown mass and force disturbance, the coefficient of energy absorption efficiency decreases along with an increase in the time constant of the piezoelectric valve (from $\eta = 0.809$ for $T_v = 0.5$ ms to $\eta = 0.629$ for $T_v = 4$ ms). As was expected, in the case of leakage disturbance we obtained smaller impact absorption efficiency for the semi-active (SA) control system than for the active (ACT) control system with gas pumping ($\eta = 0.461$ and $\eta = 0.533$, respectively). Moreover, the examples involving disturbance identification disclose $\eta = 0.492$ for the semi-active system with leakage identification (SA+I) and $\eta = 0.660$ for the active system with leakage identification (ACT+I). Let us note that the increase in absorber efficiency caused by leakage identification is much larger for active systems due to the possibility of the immediate start of gas pumping just after leakage detection. Eventually, the increase of the weighting coefficient of the control cost q causes a decrease in impact absorption effectiveness. The coefficient of impact absorption efficiency for the system with control cost is bounded by the values corresponding to semi-active and active systems ($\eta = 0.492$ and $\eta = 0.660$, respectively).

Table 2

Comparison of the coefficients of impact absorption efficiency for the considered systems

A. System with unknown mass and disturbance force				
T_v [ms]	0.5	2	4	
η	0.809	0.722	0.629	
B. System with leakage				
Control type	SA	ACT	SA+I	ACT+I
η	0.461	0.533	0.492	0.660
C. System with control cost				
q	$50 \cdot 10^{12}$	$140 \cdot 10^{12}$	$10\,000 \cdot 10^{12}$	
η	0.660	0.589	0.492	

Although all computed coefficients of impact absorption efficiency are much smaller than 1, they are significantly larger than for the passive system with a constant valve opening area. In such cases, the unexpected fluid leakage causes the impact of the piston against the cylinder bottom, which corresponds to a drastic increase in generated reaction force F_{\max} and a significant decrease in coefficient η .

5. CONCLUSIONS

In this contribution, the problem of optimal mitigation of impact excitation involving an object of unknown mass and process disturbances was formulated as an optimal control problem

with the objective function including the integral error of state-dependent path-tracking, and integral cost of control. The novel EIPC method, which combines the concepts of adaptive control and model predictive control, was proposed for an effective solution to the above impact mitigation problem. In the proposed method the identification of system and disturbance parameters is used to update the applied predictive model, while measurements of system kinematics are used to update the control problem solved at each control step. The numerical efficiency is provided by the shortening of prediction intervals and the application of simple parametrization of the control function.

The presented numerical examples, which concern the application of the EIPC for pneumatic absorbers equipped with piezoelectric valves, revealed important features of the proposed control method. They also allowed us to determine the valve parameters required for the efficient operation of the impact mitigation system. In particular, it was shown that valve time constant and maximal valve area are crucial for the realization of the path-tracking process, and their critical values for the assumed impact conditions were found. Moreover, the advantage of active control with gas pumping over semi-active control was presented and a large positive influence of real-time identification of leakage on the operation of both control methods and system efficiency was demonstrated. Finally, the influence of the weighting coefficient of the control cost term and the problem of its proper choice was discussed. It can be concluded that the EIPC proved to be an efficient and robust control method for optimal mitigation of unknown impacts. Due to its versatility and relatively low numerical cost, it seems to be applicable in various engineering applications.

The future research of the authors will be oriented towards practical implementation and detailed experimental testing of the EIPC control method. The research in this field is associated with the following challenges: i) construction of the piezoelectric stack with an embedded strain gauge to be used in the proportional piezoelectric valve; ii) application of the auxiliary controller providing a desired extension of the stack and required valve opening area; iii) implementation of the proposed control method including disturbance identification and control signal optimization on the hardware controller; iv) experimental testing of the EIPC method for various impact conditions and types of disturbances at the laboratory drop testing stand.

ACKNOWLEDGEMENTS

The support of the National Science Centre, Poland, granted through the Agreement 2018/31/D/ST8/03178, and the National Centre for Research and Development (NCBiR) granted through the Agreement LIDER/13/0063/L-10/18/NCBR/2019 is gratefully acknowledged.

REFERENCES

- [1] J. Richert, D. Coutellier, C. Götz, and W. Eberle, "Advanced smart airbags: The solution for real-life safety?," *Int. J. Crashworthiness*, vol. 12, pp. 159–171, 2007, doi: [10.1080/13588260701433461](https://doi.org/10.1080/13588260701433461).

- [2] W. Grzesikiewicz and M. Makowski, "Semi-Active System of Vehicle Vibration Damping," *Appl. Sci.*, vol. 11, no. 10, p. 4577, 2021, doi: [10.3390/app1110457](https://doi.org/10.3390/app1110457).
- [3] M.-H. Noh and S.-Y. Lee, "Parametric impact performances in a new type crash cushion barrier system using an energy absorption pipe," *Int. J. Crashworthiness*, vol. 25, no. 1, pp. 106–119, 2020, doi: [10.1080/13588265.2018.1524548](https://doi.org/10.1080/13588265.2018.1524548).
- [4] M. Huang, "Analysis of Rocket Modelling Accuracy and Capsule Landing Safety," *Int. J. Aeronaut. Space Sci.*, vol. 23, pp. 392–405, 2022, doi: [10.1007/s42405-021-00439-y](https://doi.org/10.1007/s42405-021-00439-y).
- [5] L. Fu, S. Chen, X. Bai, and J. Wang, "Optimal control of aircraft landing gear state feedback based on magneto rheological damper," *Chinese Control And Decision Conference CCDC 2018*, China, 2018, pp. 6673–6676, doi: [10.1109/ccdc.2018.8408306](https://doi.org/10.1109/ccdc.2018.8408306).
- [6] C. Graczykowski and J. Holnicki-Szulc, "Protecting Offshore Wind Turbines Against Ship Impacts by Means of Adaptive Inflatable Structures," *Shock. Vib.*, vol. 16, no. 4, pp. 335–353, 2009, doi: [10.3233/SAV-2009-0473](https://doi.org/10.3233/SAV-2009-0473).
- [7] X. Lei, G. Zhang, S. Li, H. Qian, and Y. Xu, "Dual-spring AGV shock absorption system design: Dynamic analysis and simulations," *IEEE Int. Conf. Robot. Biomim. ROBIO 2017*, Macao, 2017, pp. 1068–1074, doi: [10.1109/ROBIO.2017.8324559](https://doi.org/10.1109/ROBIO.2017.8324559).
- [8] Y. Chen, W. Chiu, and Y. Chen, "Effect of the Shock Absorber of the Shock Absorption Benefits for Upper Arm," in: Kim K., Kim H. (eds.) *Mobile and Wireless Technology ICMWT 2018*. Lecture Notes in Electrical Engineering, vol. 513, Springer, Singapore, 2019.
- [9] S. Ochelski, P. Bogusz, and A. Kiczko, "Static axial crush performance of unfilled and elastomer-filled composite tubes," *Bull. Pol. Acad. Sci. Tech. Sci.*, vol. 60, no. 1, pp. 37–43, 2012, doi: [10.2478/v10175-012-0007-8](https://doi.org/10.2478/v10175-012-0007-8).
- [10] M. Fanton *et al.*, "Variable area, constant force shock absorption motivated by traumatic brain injury prevention," *Smart Mater. Struct.*, vol. 29, no. 8, p. 085023, 2020, doi: [10.1088/1361-665X/ab905f](https://doi.org/10.1088/1361-665X/ab905f).
- [11] C. Han, B.-H. Kang, S.-B. Choi, J.M. Tak, and J.-H. Hwang, "Control of landing efficiency of an aircraft landing gear system with magnetorheological dampers," *J. Aircr.*, vol. 56, pp. 1980–1986, 2019, doi: [10.2514/1.C035298](https://doi.org/10.2514/1.C035298).
- [12] M. Shou *et al.*, "Hybrid modeling of the nonlinear behaviors for magnetorheological energy absorber," *Int. J. Mech. Sci.*, vol. 243, p. 107820, 2022, doi: [10.1016/j.ijmecsci.2022.107820](https://doi.org/10.1016/j.ijmecsci.2022.107820).
- [13] Z. Lou, R.D. Erwin, C.B. Winkler, and F.E. Filisko, "An electro-rheologically controlled semi-active landing gear," *SAE Transactions Sec. J. Aerosp.*, vol. 102, pp. 334–42, 1993, doi: [10.4271/931403](https://doi.org/10.4271/931403).
- [14] G. Mikułowski, R. Wiszowaty, and J. Holnicki-Szulc, "Characterization of a piezoelectric valve for an adaptive pneumatic shock absorber," *Smart Mater. Struct.*, vol. 22 pp. 125011–1–12, 2013, doi: [10.1088/0964-1726/22/12/125011](https://doi.org/10.1088/0964-1726/22/12/125011).
- [15] K. Zhang, S.-T. Cui, Y.-C. Chen, and Z.P. Tang, "Hydraulic shape memory alloy shock absorber: design, analysis, and experiments," *J. Intell. Mater. Syst. Struct.*, vol. 29, pp. 1986–94, 2018, doi: [10.1177/1045389X18758177](https://doi.org/10.1177/1045389X18758177).
- [16] P. Bartkowski, H. Bukowiecki, F. Gawiński, and R. Zalewski, "Adaptive crash energy absorber based on a granular jamming mechanism," *Bull. Pol. Acad. Sci. Tech. Sci.*, vol. 70, no. 1, p. e139002, 2022, doi: [10.24425/bpasts.2021.139002](https://doi.org/10.24425/bpasts.2021.139002).
- [17] A. Mackojc, B. Chilinski, and R. Zalewski, "Preliminary research of a symmetrical controllable granular damper prototype," *Bull. Pol. Acad. Sci. Tech. Sci.*, vol. 70, no. 3, p. e141002, 2022, doi: [10.24425/bpasts.2022.141002](https://doi.org/10.24425/bpasts.2022.141002).
- [18] S. Guo, L. Xu, Y. Liu, X. Guo, and L. Zuo, "Modeling and Experiments of a Hydraulic Electromagnetic Energy-Harvesting Shock Absorber," *IEEE-ASME Trans. Mechatron.*, vol. 22, no. 6, pp. 2684–2694, 2017, doi: [10.1109/TMECH.2017.2760341](https://doi.org/10.1109/TMECH.2017.2760341).
- [19] R.A. Oprea, M. Mihailescu, A.I. Chirila, and I.D. Deaconu, "Design and efficiency of linear electromagnetic shock absorbers," in *13th Int. Conf. on Optimization of Electrical and Electronic Equipment OPTIM 2012*, Romania, pp. 630–634, doi: [10.1109/OPTIM.2012.6231813](https://doi.org/10.1109/OPTIM.2012.6231813).
- [20] S. Sivakumar and A. Haran, "Mathematical model and vibration analysis of aircraft with active landing gears," *J. Vib. Control*, vol. 21, no. 2, pp. 229–245, doi: [10.1177/1077546313486908](https://doi.org/10.1177/1077546313486908).
- [21] G.L. Ghiringhelli, "Testing of semi-active landing gear control for a general aviation aircraft," *AIAA J. Aircraft*, vol. 37, no. 4, pp. 606–616, 2000.
- [22] G. Mikułowski and Ł. Jankowski, "Adaptive landing gear: optimum control strategy and potential for improvement," *Shock Vib.*, vol. 16, pp. 175–194, 2009, doi: [10.3233/SAV-2009-0460](https://doi.org/10.3233/SAV-2009-0460).
- [23] R. Faraj, C. Graczykowski, and J. Holnicki-Szulc, "Adaptable pneumatic shock absorber," *J. Vib. Control*, vol. 25, no. 3, pp. 711–721, 2019, doi: [10.1177/1077546318795532](https://doi.org/10.1177/1077546318795532).
- [24] C. Graczykowski and R. Faraj, "Development of control systems for fluid-based adaptive impact absorbers," *Mech. Syst. Signal Process.*, vol. 122, pp. 622–641, 2019, doi: [10.1016/j.ymsp.2018.12.006](https://doi.org/10.1016/j.ymsp.2018.12.006).
- [25] R. Faraj and C. Graczykowski, "Hybrid prediction control for self-adaptive fluid-based shock-absorbers," *J. Sound Vib.*, vol. 449, pp. 427–446, 2019, doi: [10.1016/j.jsv.2019.02.022](https://doi.org/10.1016/j.jsv.2019.02.022).
- [26] R. Faraj, G. Mikułowski, and R. Wiszowaty, "Study on the state-dependent path-tracking for smart pneumatic shock-absorber," *Smart Mater. Struct.*, vol. 29, no. 11, p. 115008–1–16, 2020, doi: [10.1088/1361-665X/ab9adc](https://doi.org/10.1088/1361-665X/ab9adc).
- [27] X. Zeng, G. Li, G. Yin, D. Song, S. Li, and N. Yang, "Model predictive control-based dynamic coordinate strategy for hydraulic hub-motor auxiliary system of a heavy commercial vehicle," *Mech. Syst. Signal Process.*, vol. 101, pp. 97–120, 2018, doi: [10.1016/j.ymsp.2017.08.029](https://doi.org/10.1016/j.ymsp.2017.08.029).
- [28] X. Sun, C. Yuan, and Y. Cai, "Model predictive control of an air suspension system with damping multi-mode switching damper based on hybrid model," *Mech. Syst. Signal Process.*, vol. 94, pp. 94–110, 2017, doi: [10.1016/j.ymsp.2017.02.033](https://doi.org/10.1016/j.ymsp.2017.02.033).
- [29] C. Graczykowski and R. Faraj, "Identification-based predictive control of semi-active shock-absorbers for adaptive dynamic excitation mitigation," *Meccanica*, vol. 55, no. 12, pp. 2571–2597, 2020, doi: [10.1007/s11012-020-01239-6](https://doi.org/10.1007/s11012-020-01239-6).
- [30] J. Warrick and C. Lee, "Advanced airbag system for cargo air-drop," *16th AIAA Aerodynamic Decelerator Systems Technology Conf. and Seminar*, Boston, USA, 2001, p. 293–303.